

COMPOSITION AND CONDUCTION MECHANISM OF THE NASICON STRUCTURE
X-RAY DIFFRACTION STUDY ON TWO CRYSTALS AT DIFFERENT TEMPERATURES

Heinz Kohler and Heinz Schulz
Max-Planck-Institut für Festkörperforschung, Stuttgart 80
Federal Republic of Germany

Oleg Melnikov
A. V. Shubnikov Institute for Crystallography, Moscow, USSR

(Received June 24, 1983; Communicated by A. Rabenau)

ABSTRACT

The results of a single crystal X-ray structure determination of NASICON at 495K are presented. The crystal symmetry is rhombohedral at this temperature, but monoclinic at room temperature. The structure refinement yielded the following composition: Na/3.1/Zr/1.78/Si/1.24/P/1.76/O/12/. This compound with NASICON structure is not located on the NASICON section given in the literature and this leads us to propose a new compositional plane. The conduction path involves both sodium sites and could be unambiguously derived from the joint probability density (PDF) of the Na ions. The potential barrier calculated from the PDF has about the same value as the activation energies measured on NASICON ceramics above the phase transition. These results are compared with similar studies on a pure Si NASICON crystal at temperatures up to 933K where the same conduction mechanism is found.

Introduction

NASICON ($\text{Na}/1+x/\text{Zr}/2/\text{Si}/x/\text{P}/3-x/\text{O}/12/$; $0 < x < 3$) is a solid solution system and stands for a series of compounds, which are now extensively studied because of their possible application as solid electrolytes in high temperature Na/S batteries (1). In the composition range $1.8 < x < 2.4$ these compounds have been reported to be one of the best sodium ionic conductors (2) exhibiting a conductivity between .2 and .3 (ohm cm)⁻¹ (3) at T=573K.

In this range the symmetry of the structure is monoclinic at room temperature (space group C2/c). At temperatures above 423K a phase transition to rhombohedral symmetry (space group R $\bar{3}c$) was found (4). Outside ($0 < x < 1.8$ and $2.4 < x < 3$) the solid solutions show rather poor ionic conductivity and have rhombohedral symmetry already at room temperature.

Up to now only single crystal structure investigations of the end members ($x=0$ and $x=3$) have been carried out (5,6,7), because no monoclinic single crystals were available. All structure investigations on highly conducting samples were based on powder diffraction methods and these yielded only a poor resolution of the structural details.

Experimental

We succeeded for the first time in growing single crystals of NASICON with monoclinic symmetry at room temperature. Details of crystal growth will be published elsewhere. Crystals with a maximum edgelenhth of about 0.1mm were obtained. The symmetry of the samples was first investigated with a Guinier-Simon powder camera at temperatures of 293K, 421K and 453K. The reflection pattern at 453K could be indexed in the rhombohedral space group $R\bar{3}c$. At lower temperatures several reflections were split. This splitting corresponds to a phase transition from rhombohedral to monoclinic symmetry ($C2/c$) (8).

On a single crystal with size $0.04 \times 0.04 \times 0.09 \text{ mm}^3$ intensity measurements were carried out at $T = 495\text{K}$ with an automatic X-ray diffractometer (step-scan method, $\theta/2\theta$ scan, scan width = 0.6° , $\text{MoK}\alpha$ radiation, $(\sin\theta/\lambda)_{\text{max}} = 0.75 \text{ \AA}^{-1}$). Only measurements at temperatures above the phase transition were possible, because all investigated crystals were twinned below the transition temperature which was determined to $458(10)\text{K}$. 756 symmetry unrelated reflections were measured and 454 reflections with $I/\sigma(I) > 3$ were used in the structure refinement, which included anharmonic temperature factors up to the 6th order (9). The refinement lead to a final reliability value $R_w = 0.017$ and a goodness of fit of 1.76. The refined structure parameters are presented in table I and II. Measurements on the pure Si end member of NASICON were carried out at room temperature, 403K, 593K, 788K, and 933K (table III). The results of the measurements at room temperature and 403K have already been published (10).

TABLE III

Some Experimental Data of the Diffraction Investigations on the NASICON Compound $x=3$

Temperature [K]	Number of symmetry unrelated reflections	Maximum of $\sin\theta/\lambda$ [\AA^{-1}]	R_w
298	481	.70	.018
403	687	.79	.015
593	871	.85	.020
788	857	.85	.019
933	818	.85	.019

Structure Investigation and Chemical Composition

The general feature of the NASICON structure has already been described (2,5,6). A three-dimensional network is formed by ZrO_6 -octahedra and $(\text{Si,P})\text{O}_4$ -tetrahedra, which share corners. This network has essentially two different sodium sites. The Na1 site lies in a distorted NaO_6 -octahedron and the other (Na2) site in a cage formed by 10 oxygen ions with Na2-O bond lengths between 2.5 \AA and 3.3 \AA (for $x=3$ at room temperature).

The results of our single crystal studies are as follows: In the crystal, having monoclinic symmetry at room temperature, Si is partly replaced by P. The substitution of P for Si in the tetrahedral sites is assumed to be statistical. Average bond lengths amount to $(\text{Si,P}) - \text{O1} = 1.571(3)\text{\AA}$ and $(\text{Si,P}) - \text{O2} = 1.552(4) \text{ \AA}$. The occupational disorder causes a positional disorder of the oxygens, which is displayed in high (pseudo) temperature factors. They were refined anharmonically up to the 4th order.

The refinement of the sodium sites included anharmonic temperature factors up to the 6th order. Both sites were found to be underoccupied (table I) with a surprisingly low occupation of the Na1 site. Difference Fourier maps showed no additional sodium site.

TABLE I

Positional Parameters of the Structure $x=1.24$ at $T=495K$

Site	Occup.	$x(\sigma)$	$y(\sigma)$	$z(\sigma)$
Na1	.674(13)	0	0	0
Na2	.805(8)	-.3734(3)	0	1/4
Zr	.891(3)	0	0	.14845(2)
(Si,P)	1.	.2911(1)	0	1/4
01	1.	.1944(4)	.1732(4)	.0911(2)
02	1.	.1768(4)	-.0281(5)	.1963(2)

As in the previously reported structure investigation of NASICON with $x=3$ (10) the Zr site was found to be only partially occupied (table I). This underoccupation contradicts the composition formula for NASICON: $Na/1+x/Zr/2/Si/x/P/3-x/0/12/$, reported in (2,3,4). Assuming this formula, x can be determined in two ways:

- The occupation probabilities of the sodium sites give a value of 2.1, but the resulting composition formula $Na/3.1/Zr/1.78/Si/2.1/P/0.9/0/12/$ would not lead to a balanced sum of valences.
- From the average (Si,P)-O bondlength we get a value of 1.24 (see e.g. the investigations of Jones (11) on feldspars) assuming $P-O = 1.52\text{\AA}$ and $Si-O = 1.62\text{\AA}$ (5,10,12).

In the second case the sum of valences is balanced because the lack of Zr is compensated by an excess of Na. This contradiction between both determinations of x can only be removed if the formula for the NASICON section given above is extended to a plane in the quaternary phase system (fig. 1). Then the Na con-

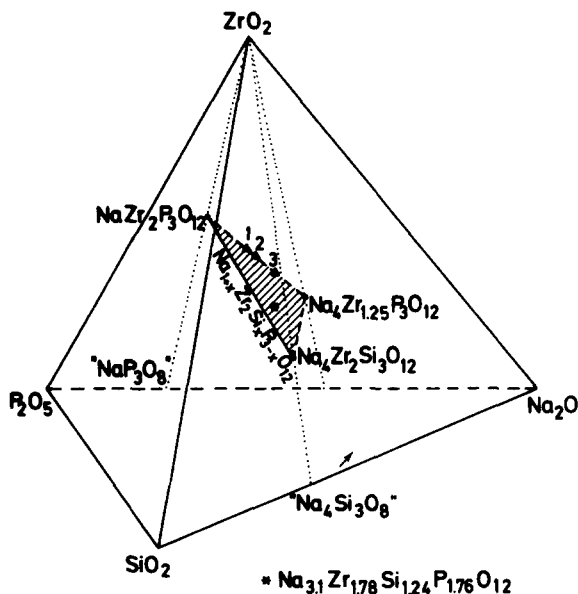
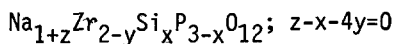


FIG. 1

Composition field of the NASICON structure as derived from structural investigations. The compositions $Na/5/Zr/4/(PO_4)/7/$ [1], $Na/7/Zr/5/(PO_4)/9/$ [2] and $Na/2/Zr/(PO_4)/2/$ [3] have already been reported (13).

tent is generally not only determined by the Si/P ratio, but also by the Zr content. This new composition plane for the compounds with NASICON structure can be described by the following formula:



The parameters x, y and z are limited by valence compensation and structural features to:

$$0 \leq x \leq 3, 0 \leq y \leq 3/4, 0 \leq z \leq 3$$

From the occupation probability of the Zr site we get $y = 0.22$. It is assumed, that the Zr site cannot be occupied by Na.

Up to now only 6 compounds located in the new composition plane have been reported. Except for the one reported here all have rhombohedral symmetry at room temperature. In addition to the well known NASICON end members ($x=0,3$) Hong reported three compounds (table I (13)) without any Si content but with lack of Zr (fig. 1).

Conduction Mechanism

The anisotropy and magnitude of the temperature factors of the Na ions (table IV) are both extremely high (fig. 2). The underoccupation, as well as the high vibrational amplitudes, indicate that both sites are involved in the conduction mechanism. This was proven with the aid of the joint probability density function ($\text{PDF}(\bar{x})$), which is given by the formula (14):

$$\text{PDF}(\bar{x}) = \sum_i w_i \text{pdf}_i(\bar{x})$$

- \bar{x} : positional vector in the elementary cell
 w_i : occupation of site i
 $\text{pdf}_i(\bar{x})$: probability density function of site i (Fourier transform of the temperature factors).
 $\text{PDF}(\bar{x})$: probability to find an atom (here Na) in a volume element of a crystal.

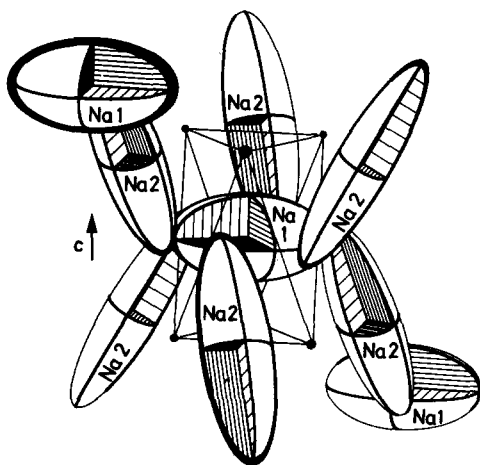


FIG. 2

ORTEP plot of the vibrational ellipsoids (20% probability) of the Na ions in relation to the NaO_6 -octahedron ($x=1.24, T=495\text{K}$). The O1 atoms are only drawn as dots.

The PDF(\vec{x}) of the sodium ions is shown in two different sections (fig. 3 and fig. 4). In fig. 3 every Na2 site is connected with the Na1 site at the center and also directly with another Na2 site. This suggests two different diffu-

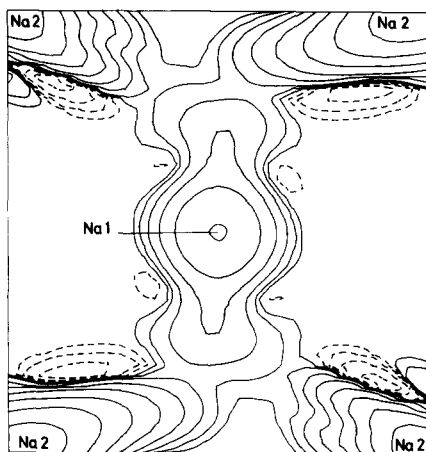


FIG. 3

Diffusion paths of the Na ions drawn in a plane including 5 Na positions. The line elevation of PDF(\vec{x}) is plotted on a logarithmic (\ln) scale. Unphysical negative values are drawn as broken lines.

sion paths. However, diffusion from Na2 to Na1 is more probable than from Na2 to Na2. Although a connection between the sodium sites is shown in fig. 3, the most probable path lies in another plane (shown in fig. 4) and does not follow a straight line. In this plane the minimum value of PDF(\vec{x}) along the path Na1 to Na2 is much higher than the corresponding minima between Na1-Na2 and Na2-Na2 in fig. 3. PDF(\vec{x}) was calculated in other sections to check whether the density directly between two Na2 sites (fig. 3) indicates a second diffusion path or is caused only by superposition of the two paths Na1-Na2. No further connection was found and we conclude that a direct jump Na2-Na2 is improbable but not impossible. Negative values of PDF(\vec{x}) are meaningless and give a rough estimation of the error in these maps.

The effective one particle potential $V_{Na}(\vec{x})$ of the sodium ions along the diffusion path was calculated according to the following relation (15):

$$V_{Na}(\vec{x}) = V_0 - kT \ln(\text{PDF}(\vec{x}))$$

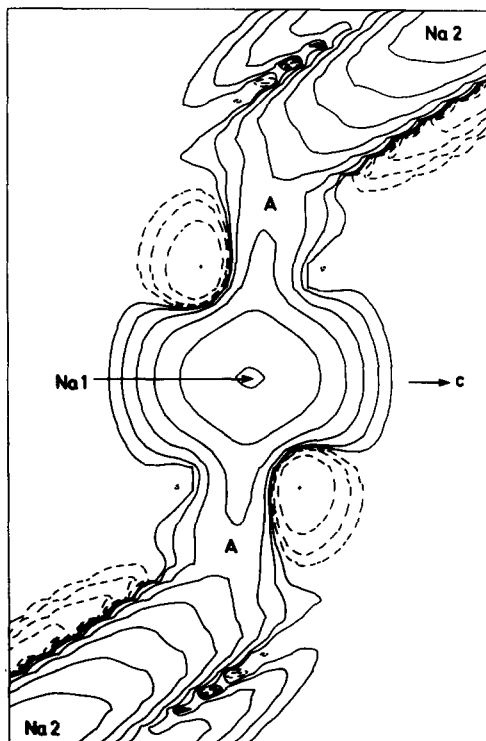


FIG. 4

Diffusion path Na2-Na1-Na2. The points A represent the minimum of PDF(\vec{x}). Details as in fig. 3.

The scaling value V_0 is determined by the absolute maximum of $\text{PDF}(\bar{x})$. At this point one sets the zero point of $V_{\text{Na}}(\bar{x})$. Comparing $V_{\text{Na}}(\bar{x})$ with structural properties reveals some interesting features of the conduction mechanism. Every Na1 ion is connected with the surrounding Na2 sites by six diffusion channels. The geometrical bottleneck for the diffusion is a triangle formed by the oxygens of the NaO_6 octahedra (fig. 2) and not a "hexagonal puckered ring" as Goodenough et al. (2) assumed. The potential barrier (minimum of $\text{PDF}(x)$) is not located at this geometrical bottleneck. This surprising fact can be understood by looking at the diameter of the bottleneck: it is 2.1Å (assuming a radius of 1.33Å for O^{2-} rigid shell) and corresponds well to the diameter of a sodium ion (12). The bottleneck therefore seems to be a favourable position for the conducting Na ions because it offers a convenient threefold Na coordination. The observed potential has a shoulder at this point (fig. 5).

The height of the potential barrier is .22eV. This is in good agreement with the activation energies of conductivity of monoclinic NASICON ceramics, which lie between .20 and .24 eV (4).

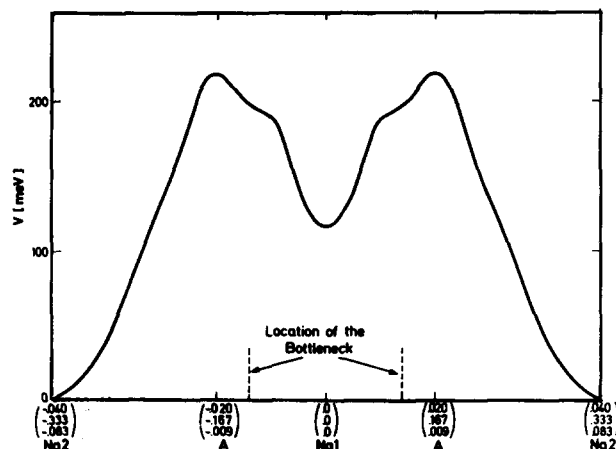


FIG. 5

Variation of $V_{\text{Na}}(\bar{x})$ along the diffusion path Na2-A-Na1-A-Na2 (compare fig. 4). The coordinates are given in brackets.

Comparison of the NASICON Structures with $x = 1.24$ and $x = 3$

The variation of the conductivity of NASICON with x (3) indicates that apart from the sodium concentration structural features may also influence diffusion.

The projections of both structures on the b,c - plane show a stretching of the NaO_6 - octahedra in the c direction for the composition $x=1.24$ as compared to $x=3$. A slight stretching was also found for the ZrO_6 -octahedra, which is partly compensated by shrinkage and rotation of the $(\text{Si,P})\text{O}_4$ tetrahedra. This leads to an increase of the c lattice constant. The c axis of the pure Si compound is considerably smaller, even at high temperatures (fig. 6). The stretching of the NaO_6 octahedra widens the bottlenecks and favours the Na mobility in the a,b -plane. As a consequence high temperature factors for the Na1 site and a low potential barrier for the diffusion from Na1 to Na2 are observed. Even at 933K the diameter of the bottleneck (1.90Å) and the rms-amplitudes of the sodium ions for $x=3$ (table IV) are smaller than for $x=1.24$ at

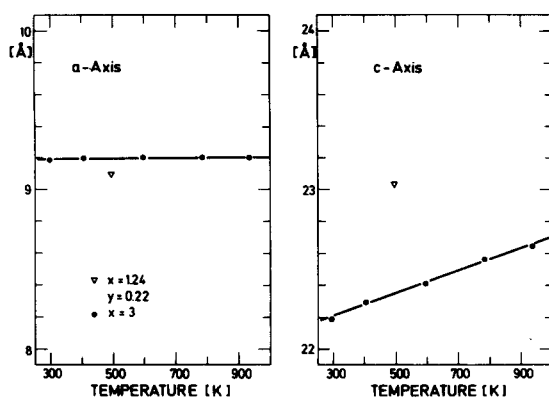


FIG. 6

Variation of the lattice constants ($x=3$) with temperature in comparison with $x=1.24$. The size of the points indicate the size of the errors.

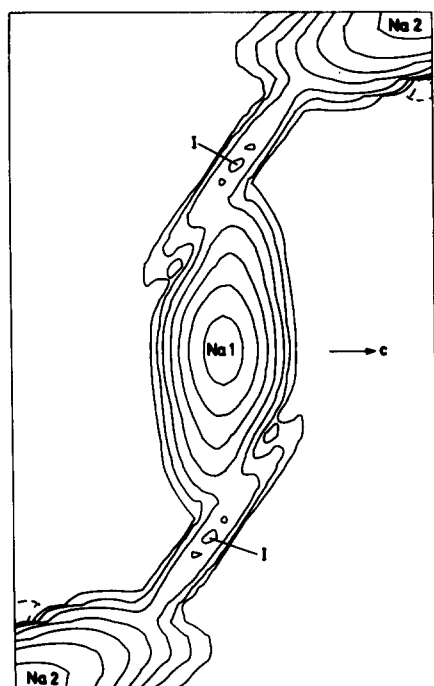


FIG. 7

Diffusion path of the sodium ions in the compound $x=3$. At I the interstitial Na ion has been introduced (occup. prob. = 0.01). Details as in fig. 3.

495K. Difference Fourier maps and $\text{PDF}(\bar{x})$ (fig. 7) show however, that the conduction mechanism is in principle the same. It includes both Na sites in contrast to the diffusion model of Tran Qui et al. (16). The bent form of the conduction path and the rather high potential barrier of the compound $x=3$ could not be described completely by anharmonic temperature factors up to 6th order only. Therefore, as a mathematical aid, an interstitial sodium site was introduced. It was refined only with anisotropic temperature factors. In agreement with the above considerations the $\text{PDF}(\bar{x})$ now shows a rather narrow conduction path and a significantly smaller expansion in the c direction at the Na1 site as compared to $x=1.24$ (fig. 7,4). From the $\text{PDF}(\bar{x})$ (fig. 7) a potential barrier of .35(8) eV was determined. An activation energy of .33eV was measured in polycrystalline samples (4).

TABLE II

Temperature coefficients of the sodium ions in the compound $x = 1.24$ at $T = 495\text{K}$. The coefficients were calculated with the Gram-Charlier expansion as described in (15).

Na2			Na1		
B_{11}	.0273(5)		B_{11}	.086(2)	
B_{22}	.0538(8)		B_{33}	.0029(2)	
B_{33}	.0183(3)		B_{12}	.043(1)	
B_{12}	.0269(4)		d_{3333}	$(2.8 \pm 1.4) \times 10^{-8}$	
B_{13}	.0135(2)		d_{1123}	$(-3.1 \pm 0.8) \times 10^{-6}$	
B_{23}	.0270(3)		f_{111111}	$(-1.06 \pm 0.09) \times 10^{-6}$	
C_{111}	$(-6.6 \pm 0.7) \times 10^{-5}$		f_{111133}	$(1.0 \pm 0.2) \times 10^{-8}$	
C_{112}	$(-7.6 \pm 0.7) \times 10^{-5}$				
C_{113}	$(-4.5 \pm 0.3) \times 10^{-5}$				
C_{133}	$(-2.6 \pm 0.2) \times 10^{-5}$				
d_{1111}	$(4.7 \pm 0.4) \times 10^{-6}$				
d_{2222}	$(32 \pm 1) \times 10^{-6}$				
d_{3333}	$(0.7 \pm 0.1) \times 10^{-6}$				
d_{1112}	$(5.1 \pm 0.4) \times 10^{-6}$				
d_{1113}	$(2.7 \pm 0.2) \times 10^{-6}$				
d_{1133}	$(2.1 \pm 0.1) \times 10^{-6}$				
d_{2223}	$(16.6 \pm 0.2) \times 10^{-6}$				
d_{2233}	$(7.3 \pm 0.2) \times 10^{-6}$				
d_{2333}	$(2.5 \pm 0.2) \times 10^{-6}$				
e_{11333}	$(0.6 \pm 0.3) \times 10^{-8}$				
e_{13333}	$(1.3 \pm 0.4) \times 10^{-8}$				
f_{111113}	$(2.0 \pm 0.6) \times 10^{-9}$				
f_{111133}	$(1.0 \pm 0.5) \times 10^{-9}$				
f_{111333}	$(-0.41 \pm 0.06) \times 10^{-9}$				

TABLE IV

Occupation and Vibration Ellipsoids of the Na Sites in both Structures investigated. The rms-Amplitudes of the other Cations are all smaller than .18 Å for $x = 1.24$ and .15 Å for $x = 3$.

Comp./Temp.	Site	Occup.	rms-Ampl. [Å]	Orient. [$^{\circ}$] of the mean axes versus cryst. axes		
				a	b	c
$x=1.24/T=495\text{K}$	Na1	.674(13)	.281(6)	90	90	0
			.52(1)	120	0	90
			.52(1)	210	90	90
	Na2	.805(8)	.18(1)	90	140	62
			.241(6)	180	60	90
			.792(4)	90	66	28
$x=3/T=933\text{K}$	Na1	.97(1)	.175(7)	90	90	0
			.396(3)	120	0	90
			.396(3)	210	90	90
	Na2	.984(7)	.172(2)	90	147	76
			.240(2)	180	60	90
			.449(3)	90	78	14

Summary and Conclusions

For the first time X-ray diffraction experiments on NASICON single crystals with monoclinic symmetry at room temperature have been carried out. Structure refinement yielded a new compositional model for the NASICON structure. It expands the NASICON phase section to a plane in the quaternary system, which includes a variation of the Zr content in the structure. Fruitless attempts of several authors (4,17,18,19) to grow crystals with compositions lying within the one dimensional NASICON phase section (2) as a single phase and the results gained from hydrothermal syntheses of compounds with $x=0$, $y>0$ (20) are a hint that compositions with a Zr deficit are more stable.

With the new detailed information on the sodium diffusion in NASICON the huge differences in conductivity with change of Si/P ratio can be better understood. The assumption of Goodenough et al. that "six channels through each NaI site provide a three dimensionally linked interstitial space" is corroborated. The bottlenecks of diffusion lie within the faces of the NaO_6 -octahedra. The width of these bottlenecks depend on composition and temperature. It is correlated with the length of the c axis. In this way diffusion is influenced by structural features. Taking this influence into account, it is better understood why the maximum in the c axis versus composition curve coincides with a sharp maximum in the conductivity (fig. 5,6 (16)). The calculated potential barriers are in good agreement with the activation energies obtained from ac measurements of polycrystalline samples.

Acknowledgement

The authors would like to thank Dr. R.Bachmann for many fruitful discussions about the presentation of this work and for careful reading of the final manuscript. We are grateful to Dr. R.Nesper for many helpful instructions to the ORTEP plotprogramm.

References

1. U. von Alpen; Dechema Monographien 92, 135 (1982); (ed. W. Vielstich, Verlag Chemie; Weinheim/Bergstr.).
2. J.B. Goodenough, H.Y-P. Hong, J.A. Kafalas; Mat. Res. Bull. 11, 203 (1976).
3. J.A. Kafalas, R.J. Cava; Proceedings "Fast Ion Transport in Solids", (Eds. Vashishta, Mundy, Shenoy), Elsevier North Holland, New York 419 (1979).
4. J.P. Boilot, J.P. Salanie, G. Desplanches, D. Le Potier; Mat. Res. Bull. 14, 1469 (1979).
5. L-O. Hagman, P. Kierkegaard; Acta Chem. Scan 22, 1822 (1968).
6. R.G. Sizova, A.A. Voronkov, N.G. Shumyatskaya, V.V. Ilyukhin, N.V. Belov; Sov. Phys. Dokl. 17, 618 (1973).
7. D. Tran Qui, J.J. Capponi, J.C. Joubert; J. of Solid State Chem. 39, 217 (1981).
8. U. von Alpen, M.F. Bell, W. Wichelhaus; Mat. Res. Bull. 14, 1317 (1979).
9. U.H. Zucker, E. Perenthaler, W.F. Kuhs, R. Bachmann, H. Schulz; J. of appl. Cryst., in the press (1982).
10. H. Kohler, H. Schulz, O. Melnikov; Mat. Res. Bull., in the press (1982).
11. J.B. Jones; Acta Cryst. B24, 355 (1968).
12. R.D. Shannon and C.T. Prewitt, Acta Cryst. B25, 925 (1969).
13. H.Y-P. Hong; Mat. Res. Bull. 11, 1973 (1976).

14. R. Bachmann; thesis, University of Karlsruhe (1983).
15. U.H. Zucker, H. Schulz; *Acta Cryst.* A38, 563 (1982).
16. D. Tran Qui, J.J. Capponi, M. Gondrand, M. Saib, J.C. Joubert; *Solid State Ionics* 3/4, 219 (1981).
17. R.J. Cava, E.M. Vogel, D.W. Johnson; *Com. of the Am. Soc.* 65, c158 (1982).
18. H. Schmid, C. de Jonghe, C. Cameron; *Solid State Ionics* 6, 57 (1982).
19. R.S. Gordon, G.R. Miller, B.J. McEntire, E.D. Beck, J.R. Rasmussen; *Solid State Ionics* 3/4, 243 (1981).
20. A. Clearfield, P. Jerus and R.N. Cotman; *Solid State Ionics* 5, 301 (1981).